Effects of Nonlinear Diode Junction Capacitance on the Nose-to-Nose Calibration*

Kate A. Remley[1], *Member, IEEE*, Dylan F. Williams[1], *Senior Member, IEEE*, Donald C. DeGroot[1], *Senior Member, IEEE*, Jan Verspecht[2], *Member, IEEE*, and John Kerley[3]

***Abstract*--We examine the effects of nonlinear diode junction capacitance on the fundamental premise of the nose-to-nose calibration, that the kickout is identical in shape to the impulse response of the sampler. We offer a physical explanation for the error introduced by the nonlinear junction capacitance in terms of small-signal diode equations.**

***Index terms*—digital sampling oscilloscope, nose-to-nose calibration, phase error, samplers.**

I. Introduction

In this letter, we show how nonlinear diode junction capacitance generates errors in the "nose-to-nose" calibration technique [1-3]. This calibration provides an estimate of the response of a broadband sampling oscilloscope, and can be used to correct measurements made with the oscilloscope. The fundamental premise of the calibration is that the sampler "kickout" pulse, which is generated at the input port of a two-diode sampling circuit when a DC offset is applied to the diode bias, is identical in shape to the sampler's time-domain "impulse response" [4].

While the error of the nose-to-nose calibration magnitude response can be estimated from power measurements of a swept-sine source [5], our options for finding the phase error are currently restricted to computational methods. References [2, 3, 6] develop an analytic model for the sampling circuit which shows that the fundamental nose-to-nose premise holds for samplers consisting of diodes with constant junction capacitance embedded in a linear network. A recent analytic method extends these models to include nonlinear diode junction capacitance [7].

Here we use numerical methods to efficiently examine many aspects of the sampling circuit behavior. We use a realistic model of a sampling circuit in SPICE, and derive a small-signal model from the large-signal behavior of the circuit. We show that the nonlinear capacitance introduces errors not accounted for in current practice, and offer a physical explanation for these errors in terms of small-signal diode equations.

[1] RF Technology Division 813.01, National Institute of Standards and Technology, 325 Broadway, Boulder, CO 80305-3328.

[2] Agilent Technologies, Inc., NMDG, VUB-ELEC, Pleinlaan 2, 1050 Brussels, Belgium.

[3] Agilent Technologies, Inc. , PO Box 2197, Colorado Springs, CO 90901-2197

II. The Nose-to-Nose Premise

A simplified representation of the sampling circuit we analyzed is shown in Fig. 1. It is based on a model for a 20 GHz oscilloscope [8, 9]. The simplified output circuit consists of a charge amplifier that sums the charge stored on the hold capacitors during each sampling cycle, as shown in Fig. 1(a).

The strobe signal forward biases the diodes during each sampling cycle. It appears differentially across the output amplifier and is cancelled. When a nonzero voltage exists at the input port and the diodes are forward biased, a net charge will transfer through the diodes to the hold capacitors. If the input and strobe signals are periodic and the strobe fires at a slightly later (or earlier) time each period, a representation of an input signal pulse will eventually be traced out by the digitized voltage samples.

We define the digitized output of the sampler in response to periodic excitation by Dirac delta functions as the "impulse response" of the sampler. For small-signal inputs, the output of the sampler can be represented by the convolution of this impulse response and the input signal [4].

The nose-to-nose premise, that the kickout pulse is identical in shape to the impulse response, can be illustrated clearly if we imagine replacing the diodes by ideal switches.

When the hold capacitor is large, the impulse response of a sampler constructed with ideal switches, rather than diodes, is a rectangular pulse[4] with the same duration as that of the switch closure, as shown in Fig. 1(a). We have no way to directly measure this impulse response, in part because we are unable to generate sufficiently sharp and well-characterized pulses. However, we can derive an estimate of the impulse response of the sampler using the nose-to-nose calibration.

When we apply a DC offset voltage to the bias lines of the diodes with no input signal applied, the hold capacitors charge if the switches are open. Each time the switches close, a pulse of the same duration as that of the switch closure will appear at the input port of the sampler, as shown in Fig. 1(b). This "kickout" pulse will be of exactly the same duration as the impulse response, but scaled in amplitude by some constant.

If we connect the input ports of our two samplers constructed with ideal switches together (nose-to-nose), the

[4] This pulse is rectangular when the RC time constant of the circuit resistance and the hold capacitor is much longer than period of the sampling window. This condition is true for the sampling circuits we investigated.

output will be the convolution of the rectangular kickout and the rectangular impulse response. This convolution, a triangular waveform of duration 2τ, is what we would measure at the output of the second sampler. A simple deconvolution process gives us τ, from which we can find the impulse response.

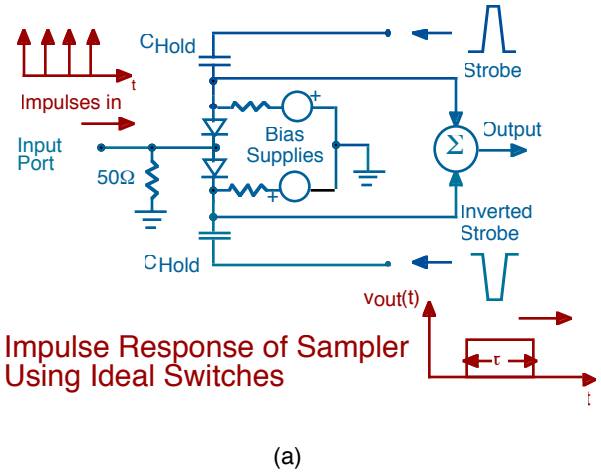

(a)

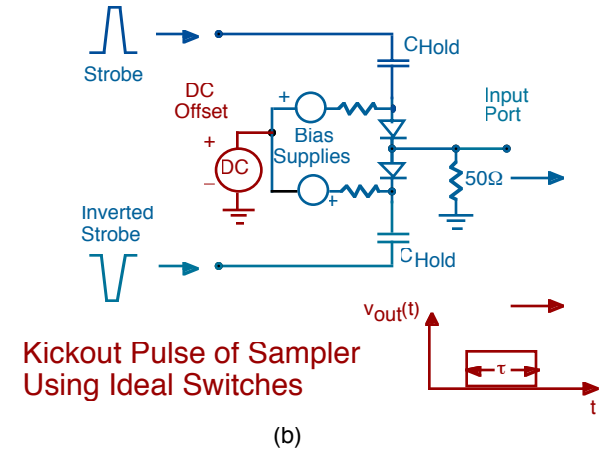

(b)

Figure 1: (a) Impulse response and (b) kickout pulse generation for a simple two-diode sampler.

When the ideal switches are replaced by diodes, the impulse response is no longer a simple rectangular function, but is altered by both the conductance function and the junction capacitance of the diodes. Nevertheless, the procedure still works if the normalized kickout and impulse responses are the same.

We can find the frequency-domain representation of the impulse response of one sampler as the square root of the output response of the second sampler. That is,

$$H_A(\omega)^{est} \cong \sqrt{K_B(\omega)H_A(\omega)}, \qquad (1)$$

where H_A is the frequency-domain representation of the impulse response of sampler A, K_B is the frequency-domain representation of the kickout pulse emanating from sampler B, and ω is the angular frequency. If $K(\omega)$ is directly proportional to $H(\omega)$, and $H_A(\omega) = H_B(\omega)$, then $H_A(\omega)^{est} = CH_A(\omega)$, where C is a proportionality constant.

Because no two samplers are identical, in practice the estimate of the impulse response of sampler A is found from a set of three measurements of three samplers. However, the calibration is still based upon the assumption that the kickout is proportional to the impulse response for each sampler.

Thus we define the error ratio E for a sampler response estimate as

$$E(\omega) \equiv \frac{H_A{}^{est}(\omega)}{H_A(\omega)} \cong \frac{\sqrt{K_B(\omega)H_A(\omega)}}{H_A(\omega)} = \sqrt{\frac{K_B(\omega)}{H_A(\omega)}}. \qquad (2)$$

III. Results

We implemented the 20-GHz sampling circuit described in [4, 8] in SPICE, neglecting any packaging parasitics, input networks, or filtering at the input of the sampler in order to concentrate on the effect of the nonlinear capacitance. We used a common model for a Schottky-barrier diode [9, 10] in which the diode conductance is in parallel with a time-varying, voltage-dependent junction capacitance. In this model, the diode's junction capacitance, $C(V_j)$, is given by

$$C(V_j) = \frac{C_{j0}}{\left(1 - \frac{V_j(t)}{\phi_{bi}}\right)^{\gamma}}, \qquad (3)$$

where C_{j0} is the zero-voltage junction capacitance, V_j is the large-signal, time-varying voltage across the diode's junction, ϕ_{bi} is the junction's built-in potential, and γ is the grading coefficient. The grading coefficient sets the amount of nonlinearity in the junction capacitance, and is typically around γ=0.5 for the type of Schottky-barrier diodes used in modern samplers [10].

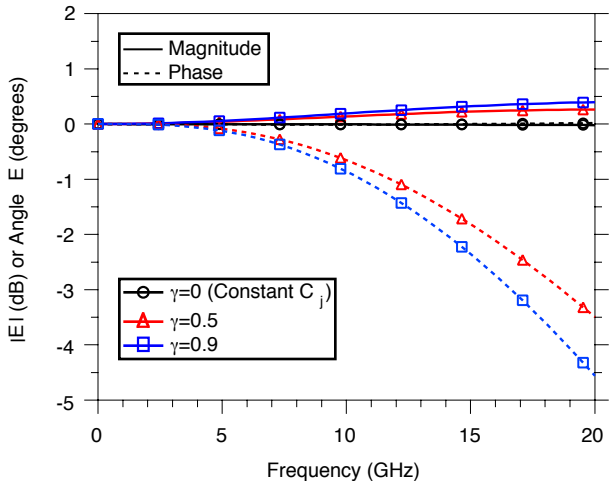

Figure 2: Increase in the error ratio E of the nose-to-nose calibration for a 20-GHz sampling circuit with increasing nonlinearity in the diode's junction capacitance.

Figure 2 shows an increase in the error of the nose-to-nose calibration as we increase the nonlinearity in the diode's junction capacitance. Note that these results cannot be extrapolated to higher frequencies since we developed the model for a 20-GHz scope. The results shown in Fig. 2 can be explained by looking at the kickout and impulse response waveforms in the time domain. Figure 3 shows that the kickout waveform rise- and fall-times are affected

by the increase in nonlinear capacitance, while we see only a minimal change in the impulse response waveform.

This broadening of the kickout pulse can be explained by considering the components of the small-signal current in the sampling diodes. For the diode model described above, the equation for the small-signal current in the diode is:

$$i(t) = g(t)v_j(t) + v_j(t)\frac{dc(t)}{dt} + c(t)\frac{dv_j(t)}{dt}. \quad (4)$$

Here $g(t)$ is the small-signal diode conductance, $c(t)$ is the diode's junction capacitance, equivalent to $C(V_j)$ in (3), and $v_j(t)$ is the small-signal junction voltage.

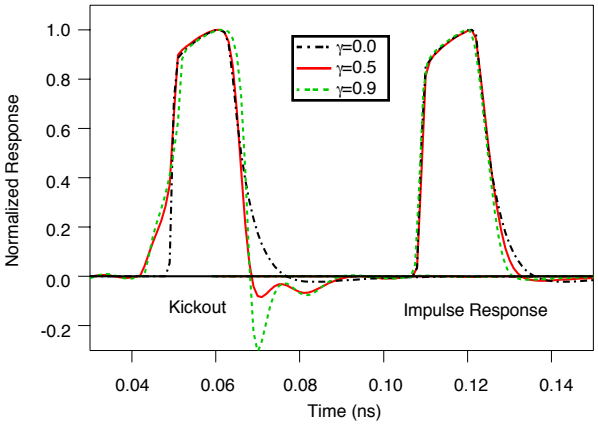

Figure 3: Kickout and impulse response waveforms for increasing nonlinearity in the diode's junction capacitance. The impulse response has been shifted in time for clarity.

Figure 4 shows the small-signal junction voltage, v_j, with nonlinear junction capacitance (γ=0.5, solid curve) and with constant junction capacitance (γ=0.0, dashed curve). This latter case is nonphysical but its impact can be assessed using SPICE. For the constant-capacitance case, v_j changes only when the diode starts to conduct, as shown in the highlighted area of Fig. 4. For the case with γ=0.5, v_j changes as the nonlinear capacitance changes. As shown by the second and third terms in (4), the time-varying quantities $c(t)$ and $v_j(t)$ give rise to a small-signal displacement current. This current causes the kickout pulse to broaden with nonlinear junction capacitance. Note that any time-varying capacitance in the sampling circuit would cause a similar effect.

The reason that the impulse response does not broaden can be understood by realizing that the kickout is proportional to the instantaneous charge on the hold capacitors, while the impulse response is reconstructed from digitized samples, each of which is generated over one complete sampling cycle. The net charge transferred to the hold capacitors through the diode capacitance over one complete sampling cycle must be zero, since no conduction current path exists through the capacitance. A new analytic model supports this conclusion [7].

IV. Conclusion

The broadening of the kickout pulse due to an increase nonlinearity of the sampling diode's junction capacitance leads to an error in the estimate of the sampler impulse response determined by the nose-to-nose calibration. While this error is not corrected in current nose-to-nose calibration methods, the effects of the error may be correctable by other means and are the subject of current research.

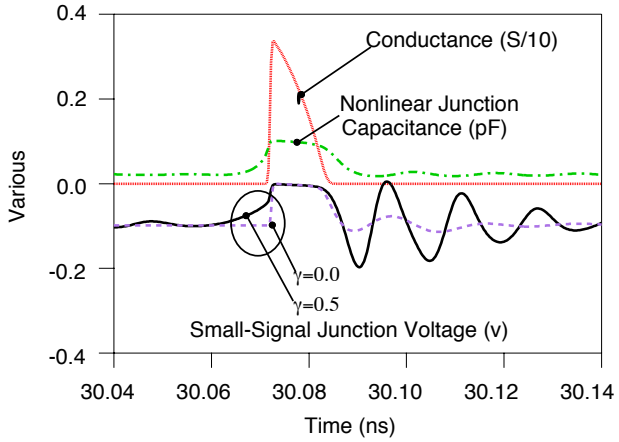

Figure 4: The small-signal junction voltage with (solid) and without (dashed) nonlinear capacitance included in the SPICE model. The small-signal diode conductance (dots) and junction capacitance (dash-dots) are included for reference. For the case with γ=0.0, the junction capacitance (not shown) is a constant of C_{j0}=0.045 pF.

References

[1] K. Rush, S. Draving, and J. Kerley, "Characterizing high-speed oscilloscopes," *IEEE Spectrum*, no. 9, pp. 38-39, Sept. 1990.

[2] J. Verspecht, "Calibration of a Measurement System for High Frequency Nonlinear Devices," Ch. 4, Ph. D. Thesis, Free University of Brussels, Brussels, Belgium, Sept. 1995.

[3] J. Verspecht, "Broadband sampling oscilloscope characterization with the 'nose-to-nose' calibration procedure: a theoretical and practical analysis," *IEEE Trans. Instrum. Meas.*, vol. 44, no. 6, pp. 991-997, Dec. 1995.

[4] D. F. Williams, K. A. Remley, and D. C. DeGroot, "Nose-to-nose response of a 20-GHz sampling circuit," in *54th ARFTG Conference Digest*, Atlanta, GA, Dec. 2-3 1999, pp. 64-70.

[5] P. D. Hale, T. S. Clement, K. J. Coakley, C. M. Wang, D. C. DeGroot, and A. P. Verdoni, "Estimating the magnitude and phase response of a 50 GHz sampling oscilloscope using the 'Nose-to-Nose' method," in *55th ARFTG Conference*, Boston, MA, June, 2000 2000, pp. 35-42.

[6] J. Verspecht and K. Rush, "Individual characterization of broadband sampling oscilloscopes with a nose-to-nose calibration procedure," *IEEE Trans. Instrum. Meas.*, vol. 43, no. 2, pp. 347-354, Apr. 1994.

[7] D. F. Williams and K. A. Remley, "Analytic Model for a Sampling Circuit," in *IEEE Trans. Microwave Theory Tech., accepted for publication*.

[8] S. Riad, "Modeling of the HP-1430A feedthrough wideband (28-ps) sampling head," *IEEE Trans. Instrum. Meas.*, vol. IM-31, no. 6, pp. 110-115, June 1982.

[9] K. A. Remley, D. C. DeGroot, and D. F. Williams, "Realistic Sampling-Circuit Model for a Nose-to-Nose Calibration," in *IEEE MTT-S International Microwave Symposium*, Boston, MA 2000, pp. 1473-1476.

[10] S. A. Maas, *Microwave Mixers*, 2nd ed. Boston, MA: Artech House, 1993.